Hemodynamics in a stented curvilinear artery

A. Pagnotta, Student number 313452, A. Paolini, Student number 308056, M.T. Santamato, Student number 316959, N. Schiavone, Student number 319632, M. Tekle, Student number 305192, D. Tkalez, Student number 318699.

***Abstract*—Currently, one of the areas of growing interest is the hemodynamics of blood vessels with complex geometries, aiming to simulate the physiological environment as closely as possible. The choice of stent type must consider the geometry of the vessel being treated. This study specifically analyzes blood flow dynamics within a curved vessel functionalized with a curved stent. The latter offers a significant advantage in terms of hemodynamic compatibility, reducing the risk of post-operative complications. Using advanced computational models, it was possible to create the vessel geometry along with its corresponding stent (CAD) and conduct analyses highlighting the optimal hemodynamics of vessels with curvature. Following a series of simulations using a Newtonian fluid with laminar flow, an appropriate mesh was selected to ensure that blood flow velocity across the section remained consistent. Parameters such as helicity and vorticity were extrapolated from the simulations, showing how these parameters are highly influenced by vessel geometries, with complex geometries potentially leading to the formation of vortices that are more pronounced near the curvature. All results underscore the importance of analysis and customization of the stent to optimize clinical outcomes. This represents a significant advancement in the field of hemodynamics and the treatment of cardiovascular pathologies.**

***Keywords*—CFD, Curvilinear, Helicity, Hemodynamic, Secondary Flow, Vorticity, WSS.**

This report was submitted for review on 3 July 2024.
Author contributions were formulated according to the CRedit (Contributor Roles Taxonomy) - https://credit.niso.org/.
The author contributions are as follows:

- A.Pag. – Writing - first draft
- A.Pao. – Software (lead)
- M.T.S. – Writing - review & editing
- N.S. – Formal Analysis
- M.T. – Project Administration
- D.T. – Software (equal)

I. Introduction

THE study of hemodynamics in arteries, particularly those with complex geometries, has gained significant attention due to its implications for cardiovascular health. Hemodynamics refers to the dynamics of blood flow within the circulatory system, which is crucial in understanding various cardiovascular diseases. The curvature of arteries and the presence of stents can significantly influence blood flow patterns, shear stress distributions, and ultimately the development of pathologies such as atherosclerosis and restenosis.

Curvilinear arteries present unique hemodynamic challenges compared to rectilinear arteries. The curvature induces secondary flows and complex vortex formations, which can alter the wall shear stress (WSS) and contribute to the progression of arterial diseases (1). Computational Fluid Dynamics (CFD) has emerged as a powerful tool to simulate blood flow in these complex geometries, providing detailed insights into hemodynamic parameters that are difficult to measure in vivo or in vitro (2).

Stenting is a common therapeutic intervention used to restore and maintain patency in stenotic arteries. However, the introduction of a stent, e.g. the Nobori stent, can further complicate the hemodynamic environment. Stents can disrupt the natural flow of blood, leading to altered WSS and potential complications such as in-stent restenosis (ISR) (3). Understanding these hemodynamic alterations is crucial for optimizing stent design and improving patient outcomes.

In this study, we conducted CFD simulations to investigate the hemodynamics in both rectilinear and curvilinear stented arterial geometry. The steady-state simulations aimed to compare the flow patterns, WSS distributions, and other hemodynamic parameters between these geometries.

Previous studies have demonstrated the efficacy of CFD in predicting hemodynamic changes due to stenting (4) (5) and this study aims to extend this knowledge by focusing on the differences between rectilinear and curvilinear arterial segments.

By providing a detailed analysis of the hemodynamics in these scenarios, this research seeks to enhance our understanding of the biomechanical environment in stented arteries, which is critical for the development of improved stent designs and better clinical outcomes.

II. METHODS

A. *CAD models and Material Properties*

For the three-dimensional geometry reconstruction of the 3D-printed Nobori stent deployed in two idealized straight and curvilinear vessels, Solidworks software is used (Fig. 1). The first stent model created was designed for implantation in the straight vessel. Then, considering the curvilinear arterial model, a cylindrical extruded tube was curved through the Flex function, imposing a radius of curvature of 56.3 mm. These geometric models represent typical arterial structures to investigate the hemodynamic effects induced by curvature. The Nobori stent was incorporated within these arterial geometries to simulate its impact on blood flow. The stent is composed of only three rings and ten crowns per ring. Dimensions used for the creation of the stents are listed in Table I.

TABLE I
NOBORI STENT DIMENSIONS

Element	Value
External diameter	3 mm
Crown angle	139.28°
Crown width	0.15 mm
Struct length	1.05 mm
Struct width	0.10 mm
Struct thickness	194.44 μm
Link length (along x)	0.27 mm
Link width	0.10 mm
Peak-to-peak longitudinal distance	2.90 mm
Ring width (along x)	0.91 mm

Values are referred to a scale factor of x3.6 mm

Blood was modeled as an incompressible non-Newtonian fluid with a density of 1060 kg/m³. The dynamic viscosity μ of blood is described using the Carreau's model, which accurately captures the rheological behavior of blood for low shear rate:

$$\mu = \mu_\infty + (\mu_\infty + \mu_0) \cdot [1 + (\lambda \cdot S)^2]^{n-1/2} \quad \textbf{(1)}$$

where S is the shear rate, μ_o and μ_∞ are the viscosity values at S equal to zero and infinite, which respectively are equal to 0.25 Pa × s and 0.0035 Pa × s, λ is the time constant equal to 25 s and n is the power-law index equal to 0.25 (6) (7).

B. *Meshing and Boundary Conditions*

A comprehensive mesh sensitivity analysis was conducted to determine the optimal balance between computational cost and solution accuracy. This analysis ensured that the CFD results were mesh-independent. Various mesh configurations were tested, as detailed in Table II.

TABLE II
MESH CONFIGURATIONS

	# 1	# 2	# 3	# 4	# 5
Min and Max global sizing (cm)	0.002 – 0.06	0.003 – 0.08	0.0045 – 0.12	0.00525 – 0.14	0.05 – 0.8
Min and Max local sizing in stented zone (cm)	0.003 – 0.08	0.003 – 0.08	0.0045 – 0.12	0.00525 – 0.14	0.05 – 0.8
Min and Max local sizing in non-stented zone (cm)	0.001 – 0.08	0.01 – 0.08	0.03 – 0.12	0.0175 – 0.07	0.1 – 0.8
Relative % difference with respect to the finest mesh		-0.372%	0.704%	0.594%	-6.337%

The final mesh selected utilized polyhedral cells in the bulk flow regions and local mesh refinement in the stented region to capture the intricate flow details. The surface mesh dimensions were as follows: global sizing ranged from 0.003 cm to 0.08 cm, local sizing in the stented zone was from 0.003 cm to 0.08 cm, and local sizing in the non-stented zone was from 0.01 cm to 0.08 cm. The volume mesh had a maximum cell length of 0.08 cm.

The simulation assumed laminar flow due to the low Reynolds number. The boundary conditions included a flow rate at the inlet, calculated using the average flow rate formula (8):

$$Q = 1.43 \cdot d^{2.55} \quad \textbf{(2)}$$

where d is the hydraulic diameter of the inlet, i.e. 10.8 mm. At the outlet, a pressure of zero was imposed. The wall surface was modeled as stationary with a no-slip condition.

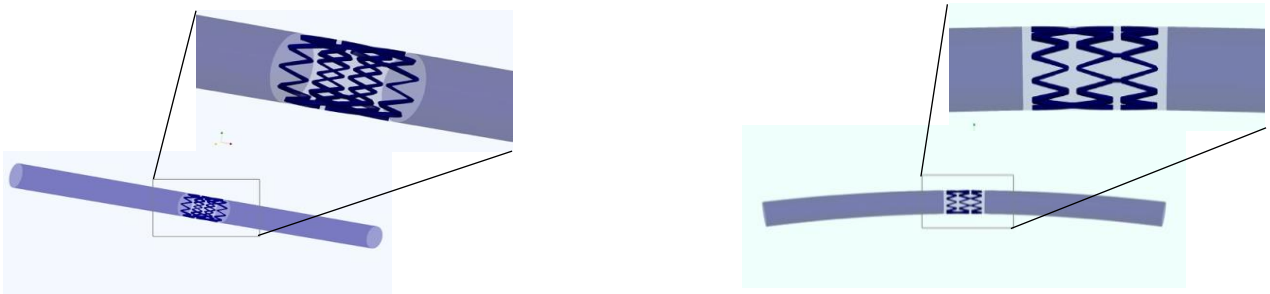

Figure 1. Straight stented artery (left) and curved stented artery (right)

C. *CFD simulation*

The CFD simulation was performed using ANSYS FLUENT. The Semi-Implicit Method for Pressure-Linked Equations-Consistent SIMPLEC scheme was adopted for Pressure-Velocity Coupling. The under-relaxation factors were set as follows: pressure equal to 0.3, density and body forces equal to 1, and momentum = 0.7. The convergence criteria were defined by an absolute residual value of 10^{-4} for continuity and all three components of the velocity.
The maximum number of iterations was set to 1000 to ensure thorough convergence of the solution. The governing equations were initialized using Standard Initialization setting pressure and velocity initial values to zero in order to provide a stable starting point for the iterative solution process.

D. *Quantities of interest*

Hemodynamics in stented rectilinear and curvilinear models was analyzed considering vorticity, helicity, wall shear stress and secondary flows to study the bulk flow and compare results obtained for straight artery and curvilinear artery.
In fluid dynamics, vorticity is a vector quantity that represents the rotation of the fluid's velocity field. It provides a measure of the local rotation of fluid particles and can be visualized as the tendency of the fluid to rotate around a point or axis. It is defined as:

$$\boldsymbol{\omega} = \nabla \times \mathbf{v} \quad (3)$$

where v is the velocity vector of the fluid.
The helicity H is a bulk-flow quantity that measures the alignment of the velocity and vorticity vectors; it has a relevant influence on the evolution and stability of laminar and turbulent flow. It is defined as the integrated internal product of the velocity field with the vorticity field:

$$\mathbf{H} = \mathbf{v} \times \boldsymbol{\omega} \quad (4)$$

Conventionally, positive values of helicity correspond to clockwise rotation, negative values correspond to counterclockwise rotation.
Then, as near-wall quantity, Wall Shear Stress was considered, which is a vector whose magnitude is equal to the viscous stress on the surface, whereas its direction describes the direction of the viscous stress acting on the surface:

$$\boldsymbol{\tau}_j = \mathbf{n} \cdot \boldsymbol{\tau}_{ij} \quad (5)$$

where $\mathbf{n}$ is the normal vector to the surface and $\boldsymbol{\tau}_{ij}$ is the fluid viscous stress tensor.
Secondary flows describe fluid movements that develop in directions that are different from the main flow's one. Their origin is strongly linked to the presence of curvatures in the vessels, where the centrifugal force resulting from the curvature tends to push the blood towards the outer part of the vessel, generating vortices and secondary flows.

III. RESULTS

In terms of *vorticity*, it is easily understandable from the Fig. 2 that it is practically zero in the case of the straight vessel, while for the curved vessel, there are significant values, especially as one moves away from the central axis of the vessel.

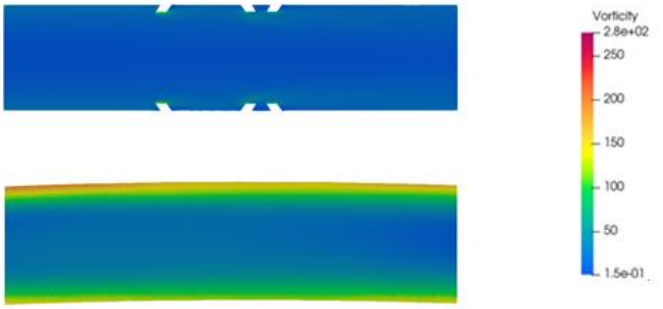

Figure 2. Vorticity in straight stented vessel (top) and curved stented vessel (bottom)

As shown in the Fig. 3, the vorticity values increase approaching the wall, exceeding 250 s^{-1}. It can therefore be assumed that, in the curved vessel, the blood particles rotate with significant speed near walls, so it is realistic to expect non-negligible stress values on these arterial walls.

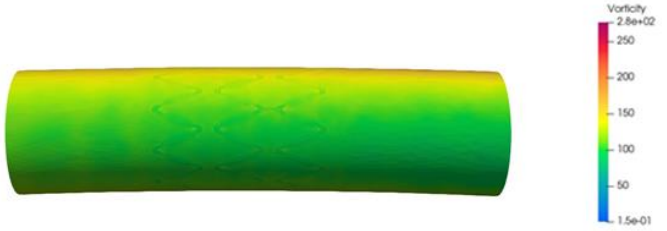

Figure 3. Vorticity near the arterial wall (curved vessel)

Considering the qualitative evaluation, it's evident that a straight stent doesn't induce significant flow *helicity* since the flow along a straight tube is typically uniform and non-torsional. As depicted in the Fig. 4a, the helicity value remains consistently close to zero. Conversely, a curved stent introduced a bend in the artery, which influenced the helicity of blood flow. This curvature resulted in either positive or negative helicity depending on its direction, as shown in Fig. 4b.

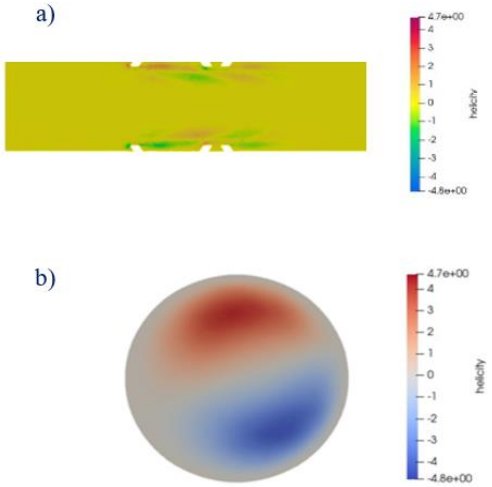

Figure 4. Helicity in longitudinal section of the straight stented vessel (a); helicity in Transverse cross-section of the curved stented vessel (b)

Towards the middle and beyond of the stent, near the tighter curve (inner curvature), negative helicity was often observed. This was due to the continuous downward curvature of the artery, causing a twist in the blood flow opposite to the curvature. Moving upwards from the middle of the stent, near the outer curve (wider curvature), positive helicity was typically observed. Here, the upward curvature of the artery induced the blood flow to curve upwards along the upper surface of the artery.

The current findings demonstrate how changes in the primary curvature of a simulated artery, implanted with a stent, affect the resulting distribution of *WSS*. The innermost curve of the curved stent, which is shorter in length, is referred to as the **myocardial** surface (inner curve), whereas the outermost curve is known as the **pericardial** surface (outer curve).
Compared to a straight stent, the distribution of WSS shows greater heterogeneity in a curved stent. Specifically, in the case of a curved stent, examination of WSS reveals that it is higher on the pericardial luminal surface compared to the myocardial luminal surface. This difference is likely due to the skewing of the velocity profile caused by the stent's curvature.
Conversely, in a straight stent, such variations are absent because WSS remains more uniform across the entire surface. In a curved stent, variations in WSS are more pronounced along the axial length, particularly in the proximal and distal transition regions of the stent. These variations are less prominent in a cylindrical (straight) stent (9).

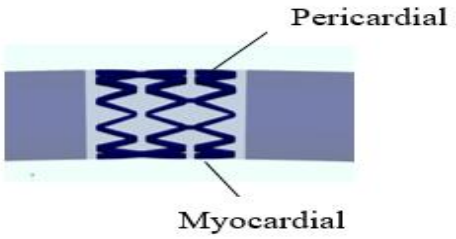

Figure 5. Pericardial and myocardial surface in a stented artery

Fig. 6 shows the comparison of *secondary flows* between the straight and curved artery: it is possible to notice the almost complete absence of secondary flows in the case of the straight artery, unlike the curved case where Dean vortices will be present (Fig. 7). This different behavior was predictable because the flow, when it reaches a curved section, is affected by the centrifugal force and becomes three-dimensional, as it has a component on the plane orthogonal to the vessel axis and a component oriented along the vessel axis itself.
It is equally interesting to see how these secondary flows vary depending on which part of the stent is being analyzed: they have both different values and orientations at the stent's entry.

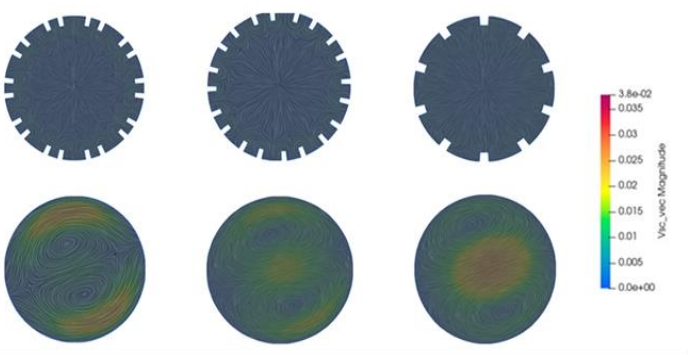

Figure 6. Transverse cross-sections, from left to right, of downstream, centre and upstream of the stent for rectilinear artery (top row) and curved artery (bottom row).

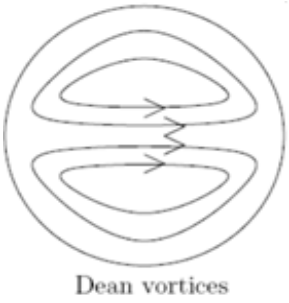

Figure 7. Transverse cross-section showing secondary flows which form Dean vortices

IV. Discussions

The results obtained from the comparison between the straight artery and the curved artery were largely predictable, as the combination of centrifugal forces, pressure gradients, and the three-dimensional nature of the flow in a curve makes the occurrence of turbulence, vorticity, and secondary flows more likely.
Moreover, it's important to keep in mind that every consideration derived from this simulations and results obtained should be interpreted with caution, because some limitations are introduced in our model.
For example, the arterial wall was assumed to be rigid, and the arterial vessel was assimilated to a cylindrical conduit with a constant circular cross-section, but we know well that vessels are not exactly circular and their cross-section varies as they move away from the heart, so each of these assumptions could result in slightly different local hemodynamics.

V. CONCLUSIONS

The complex geometries of three-dimensional stented arteries pose significant computational challenges for conducting CFD simulations. In this study, we propose employing a hybrid meshing approach aimed at achieving accurate CFD results efficiently, while optimizing the use of computational resources available.

Specifically, the curved stent was observed to introduce variations in flow patterns along its length, with distinct changes in helicity and the emergence of vorticity and secondary flows in different regions of the stent. This indicates that the geometry of the curved stent plays a crucial role in shaping blood flow dynamics and the mechanical environment experienced by the artery walls. Understanding these dynamics is essential for optimizing stent designs to enhance biocompatibility and long-term efficacy in clinical applications.

VI. REFERENCES

1. S. A. Bergereì, L. -D. Jou. *"Annual review of fluid mechanics," in Flows in stenotic arteries 15–64.* [Online]

2. 15–64, D. N. Ku. *"Annual review of fluid mechanics," in Blood flow in arteries, 15–64.* [Online] 29 1 1997.

3. P. A. Lemos, C. H. Lee, V. Aragon, J. A. Lemos. *"Clinical Outcomes and Predictoris of In-Stent Restenosis After Drug-Eluting Stent Implantation in a Real-World," Journal of the American College of Cardiology, 1741-1747, 51(18).* [Online]

4. F. Migliavacca, L. Petrini , M. Colombo, F. Auricchio, G. Dubini. *"Mechanical Behavior of Coronary Stents Investigated Through the Finite Element Method," Journal of Biomechanics,.* [Online] 2002,.

5. C. Kleinstreuer, Z. Li, M. A. Farber, 35(4), 654-670. *"Fluid-Structure Interaction of Stented Abdominal Aortic Aneurysms," Annals of biomedical engineering, 35(4), 654-670.* [Online] 2008.

6. T. Seo, L. G. Schachter, A. I. Barakat,. *"Computational study of fluid mechanical disturbance induced by endovascular stents," Annals of biomedical engineering,33: 444-456.* [Online] 2005,.

7. S. Chien, S. H. U. N. I. C. H. I. Usami, H. M. Taylor, J. L. Lundberg, M. I. Gregersen 21.1: 81-87. *"Effects of hematocrit and plasma proteins on human blood rheology at low shear rates," Journal of applied physiology 81-87.* [Online] 21 1 1966.

8. A. G. Van der Giessen, H.C. Groen, P. A. Doriot, P. J. De Feyter, A. F. Van der Steen, F. N. Van de Vosse et al. *"The influence of boundary conditions on wall shear stress distribution in patients specific coronary trees," Journal of biomechanics,.* [Online]

9. John F LaDisa, Lars E Olson, Hettrick A Douglas, David C Warltier, Judy R Kersten and Paul S Pagel. *Alterations in regional vascular geometry produced by theoretical stent implantation influence distributions of wall shear stress:.* [Online]